

RESEARCH ARTICLE | NOVEMBER 07 2023

Laser cladding: A high-speed-imaging examination of powder catchment efficiency as a function of the melt pool geometry and its position under the powder stream

Daniel Koti ; John Powell ; Himani Naestroem ; Chiara Spaccapaniccia; K. T. Voisey 



J. Laser Appl. 35, 042065 (2023)

<https://doi.org/10.2351/7.0001199>



CrossMark



Journal of
Laser Applications

Learn More



RAPID TIME
TO ACCEPTANCE



COMMUNITY
DRIVEN



EXPANSIVE
COVERAGE



PRESTIGIOUS
EDITORIAL BOARD



EXTENSIVE
MARKETING

Laser cladding: A high-speed-imaging examination of powder catchment efficiency as a function of the melt pool geometry and its position under the powder stream

Cite as: J. Laser Appl. 35, 042065 (2023); doi: 10.2351/7.0001199

Submitted: 25 July 2023 · Accepted: 19 October 2023 ·

Published Online: 7 November 2023



View Online



Export Citation



CrossMark

Daniel Koti,^{1,a)} John Powell,^{1,2} Himani Naestroem,³ Chiara Spaccapaniccia,⁴ and K. T. Voisey¹

AFFILIATIONS

¹Faculty of Engineering, University of Nottingham, University Park, Nottingham NG7 2RD, United Kingdom

²University of Stuttgart, ICM, D-70569 Stuttgart, Germany

³Department of Engineering Sciences and Mathematics, Lulea University of Technology, 97187 Lulea, Sweden

⁴Independent Researcher

^{a)}Electronic mail: daniel.koti@nottingham.ac.uk

ABSTRACT

This paper provides quantitative information about the paths taken by blown powder particles during laser cladding. A proportion of the powder is “wasted” by bouncing off the solid areas surrounding the melt pool. This wastage reduces the productivity and profitability of the process. In this paper, specially developed software was used to analyze high-speed imaging videos of the cladding process, to monitor the directions of powder particle flight toward and away from the melt pool area. This information has been correlated to the geometry and position of the melt pool zone for three different cladding techniques: single track cladding (A tracks), standard overlapping track cladding (AAA cladding), and a recently developed technique called ABA cladding. The results show that the melt pool geometry, and particularly the overlap between the melt pool and the incoming powder stream, has a strong influence on powder catchment efficiency. ABA cladding was found to have considerably better powder catchment efficiency than standard AAA cladding and this improvement can be explained by consideration of the geometries and positions of the melt pools and surrounding solid material in each case. As powder costs are an important factor in industrial laser cladding, the adaption of the ABA technique, and/or control of pool/powder stream overlap (e.g., by making the powder stream not coaxial with the laser beam), could improve the profitability of the process.

Key words: laser cladding, laser direct energy deposition, DED, powder catchment efficiency, productivity, powder stream, ABA laser cladding, high-speed imaging

© 2023 Author(s). All article content, except where otherwise noted, is licensed under a Creative Commons Attribution (CC BY) license (<http://creativecommons.org/licenses/by/4.0/>). <https://doi.org/10.2351/7.0001199>

I. INTRODUCTION

Laser cladding is a directed energy deposition (DED) technique that involves melting a blown stream of metal powder onto a substrate surface to provide a coating, which has good wear or corrosion properties.^{1–3} Unfortunately, a proportion of the powder fed into the process misses the melt pool and is not incorporated into the clad layer.⁴ This “escaping” or “wasted” powder is an important feature of the profitability of the cladding process because the

powder is expensive and generally cannot be recycled.⁵ This paper describes the results of an experimental program designed to identify the total amount of powder that escapes and the directions taken by the escaping powder particles under various process parameters as a function of melt pool geometry.

The process parameters investigated included cladding speed, intertrack distance, and cladding technique. Three cladding techniques were compared: single track cladding (“A” cladding), standard, overlapping track cladding (AAA cladding), and a recently

developed technique called ABA cladding.^{6,7} These three techniques are described in Fig. 1. High-speed imaging (HSI) videos were taken of the laser-material interaction area during cladding, and specially designed software was employed to identify the flight vectors of the individual particles toward, and away from, the melt pool.

II. EXPERIMENTAL DETAILS

A. Cladding parameters

Laser cladding experiments were conducted with the following parameters: 15 kW IPG ytterbium-doped, cw fiber laser (1070 nm wavelength), 3 kW power; 150 mm collimating lens and Kugler mirror optics with a 250 mm focusing mirror; fiber diameter, 100 μm , coupled to a 400 μm fiber; beam diameter on the substrate surface, 4 mm (Gaussian energy distribution); and stand-off distance, 13 mm.

The powder was fed through an 8 mm diameter coaxial COAX 14V5 (Fraunhofer IWS) continuous nozzle (also known as a ring-slit nozzle). This produced a focused powder stream with a diameter of approximately 4 mm at the melt pool surface. Argon was used as the shielding and carrier gas.

The carrier gas flow was 8 l/min, and the shielding gas flow was 15 l/min. 316L stainless steel powder with a size range from 50 to 150 μm diameter was fed from a gravity-based powder feeder. The powder feeder was calibrated, and the feed rate used (26 g/min) was checked experimentally and found to have a standard deviation of 0.8 g/min. A three-axis ISEL FlatCOM L150 CNC system was used, with the substrate plates (5 mm thick 304S15 stainless steel) clamped to a linear motion table. Both the laser head and the powder feeder nozzle remained fixed.

Tracks were created using both the AAA and ABA techniques with a range of intertrack (center to center, see Fig. 1) spacings between 2 and 4 mm. The tracks comparing “AAA” and “ABA” clads were carried out at 0.7 m/min. For the solo “A” track cladding experiments, the cladding speed was varied between 0.7 and 1.5 m/min, to investigate the pool shape changes as a function of process speed.

B. Powder particle trajectory image processing

HSI videos were taken of the cladding zone, and diagnostic code was written in Python using NumPy, OpenCV, and OpenPIV. The code’s operations were divided into the following steps: 1. particle detection, 2. velocity computation, 3. association of directional vectors to individual particles, and 4. computation of flow rates in different directions. The code was applied to individual HSI frames for particle detection, and pairs of consecutive images were used for the computation of displacement vectors.

The initial step is to achieve a binary image where only the particles are visible. In addition to the information on particle positions, the individual frames from the HSI contain high intensity, low-frequency signals from the deposition area, and high-frequency low-intensity electronic noise. The first was attenuated through background intensity removal, while the latter was removed by the low-pass filtering of the Fourier spectrum of the image.

The operation was repeated twice, until the particle signal became predominant, and a clear threshold could be used to binarize the image. Finally, particle counting was performed on the binary image using OpenCV structural analysis toolbox.

The algorithms used to calculate the particle vectors were PIV (particle image velocimetry) and OF (optical flow). Both algorithms were applied to the whole image and required two consecutive frames to analyze the displacement of the particles. PIV was very effective in computing vectors in high-speed regions of the image, while OF was more reliable for the regions of low particle speed. It is important to mention that the original images are used to compute displacement vectors, since using a binarized image leads to errors in the cross-correlation-based algorithm.

The steps above identify the direction and velocities in the regions of interest but do not link them to the individual particles. In order to associate a vector with every particle, it is necessary to overlap the binary image obtained in step 1 with the velocity maps obtained in step 2.

C. Mapping the geometry of the melt pool and its overlap with the powder stream

Using techniques developed in earlier work,⁷ the plan view geometry of the weld pool was accurately identified from the HSI videos. In each case, this could then be mapped onto the circular cross section of the vertically incident powder stream. From this information, it was possible to calculate the percentage of the powder stream that landed in the liquid pool and the proportion that landed on the surrounding solid material.

The powder stream was coaxial with the laser beam, and both were circular in cross section. However, it is important to point out that the melt pools were not circular, and there was generally a lag between the front edge of the melt pool and the front edge of the powder stream.

III. RESULTS AND DISCUSSION

A. Single “A” track cladding at different speeds

Figure 2 presents a single frame from the HSI video of the laser-material interaction zone in single “A” track cladding. The cladding process is moving toward the viewer in this photo. Flight vectors, calculated as described above, have been added to some particles (depicted as arrows, the length of which are proportional to speed).

It is clear from Fig. 2 that most of the descending powder stream is entering the melt pool. However, a small proportion of the particles are flying away from the area after rebounding off the solid material, which surrounds the melt. From the software analysis of the HSI video, it was possible to identify the mass of incoming powder entering the melt pool as a percentage of the total powder feed rate, and this can be expressed as the powder catchment efficiency.⁷ Figures for powder catchment efficiency can also be calculated by measuring the cross section of the clad tracks and, thus, the mass per unit time laid down in the clad layer. Both sets of results are presented in Fig. 3 and the subsequent figures.

Single track “A” cladding was carried out at a range of speeds. Figure 3 shows the plan view of the shape of the cladding melt pools for single “A” tracks at various process speeds (measured from the HSI videos) with a dotted circle identifying the position and area of the incident powder stream. Plan views of the melt pools were chosen because the input powder is effectively a vertical

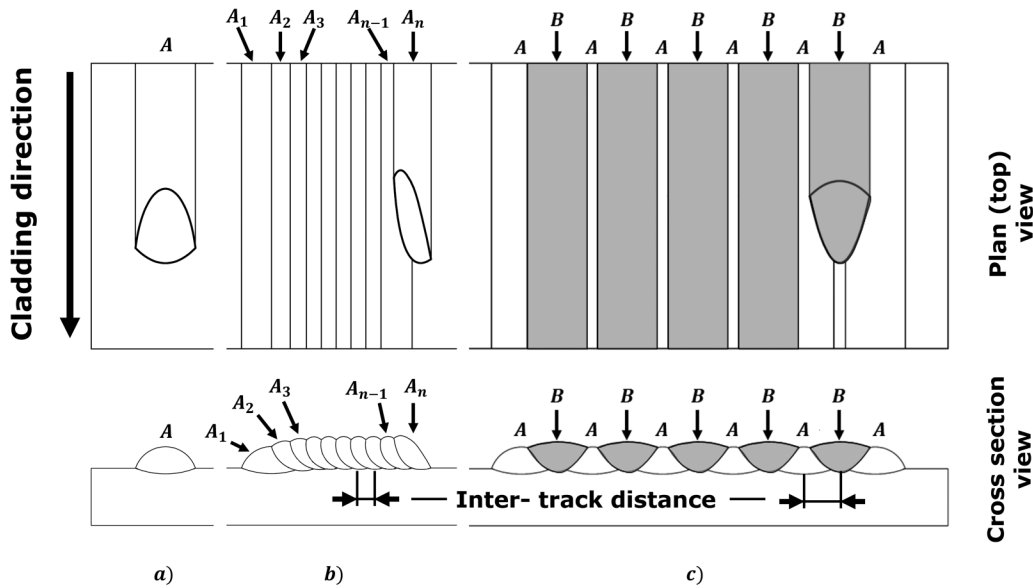


FIG. 1. (a) A solo, or initial, “A” track; (b) in standard (AAA) laser cladding, the clad surface is made up of overlapping “identical” tracks (although a few, early tracks differ from later tracks); (c) in ABA cladding, a set of widely spaced identical “A” tracks are laid down first and then the gaps between them are filled with “B” tracks.

stream. It is interesting to note that, although the range of process speeds shown here is from 0.7 m/min to over double that value (1.5 m/min), the reduction in the surface area of the pool is only 20% (from 27.2 to 21.72 mm²). It is clear that there is a gradual decrease in the powder catchment efficiency with increasing cladding speed.

In Fig. 3, the position of the powder stream for each cladding speed melt pool was established directly from the HSI video. The

figure gives the details of the melt pool area, the powder catchment efficiency, and the percentage area overlap between the powder stream and the melt pool. It can be seen that, in every case, the melt pool front lags the front of the powder jet slightly. Under some processing conditions, this would be expected because the powder jet and laser are aligned, and the cold, flat substrate would need some time/distance under the laser beam before melting is initiated.

29 November 2023 10:48:07

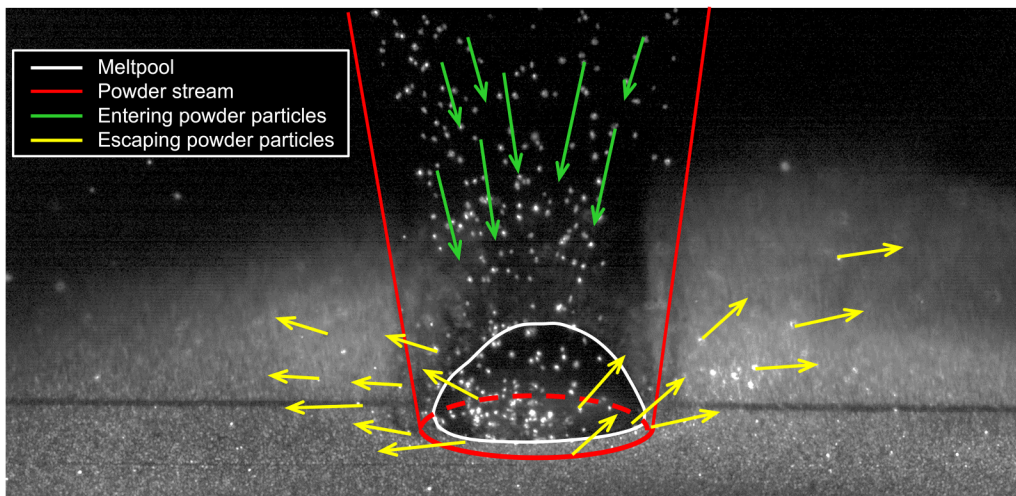


FIG. 2. A frame from the HSI video of single “A” track cladding. Selected particle vectors are shown as arrows (arrow length is proportional to speed).

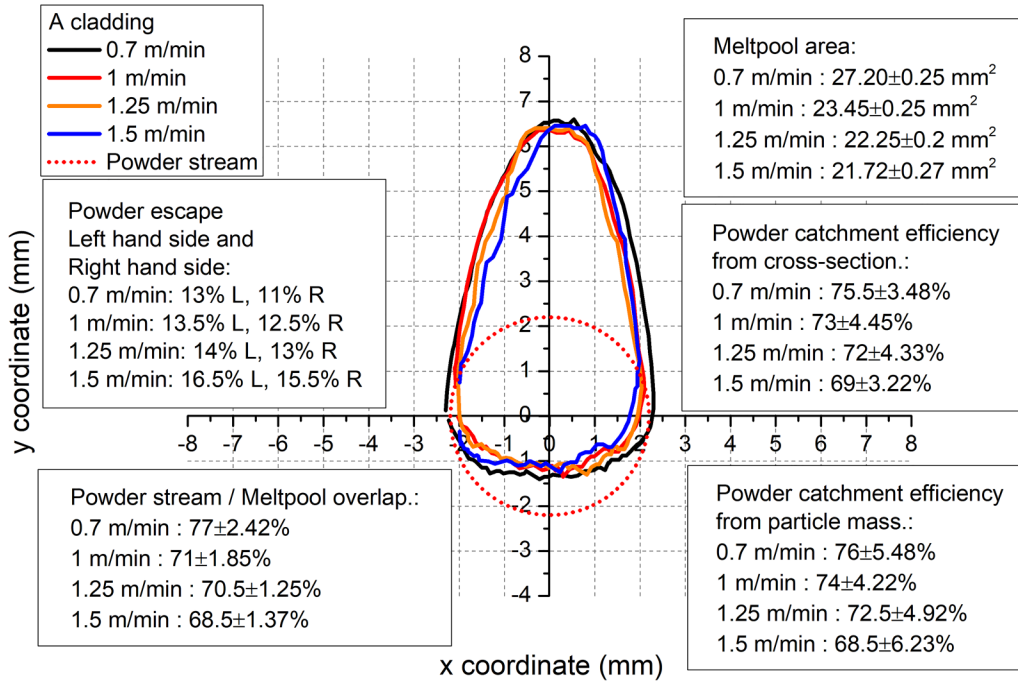


FIG. 3. Plan views of melt pools in single track “A” cladding as a function of cladding speed. The position and size of the powder stream are indicated as a dotted circle. “Powder catchment efficiency from particle mass” figures are taken from the HSI video analysis.

It is interesting to note that there is a very good match between the percentage overlap (powder/pool) and the powder catchment efficiency. The area overlap between the melt pool and the powder stream matches the powder catchment efficiency to

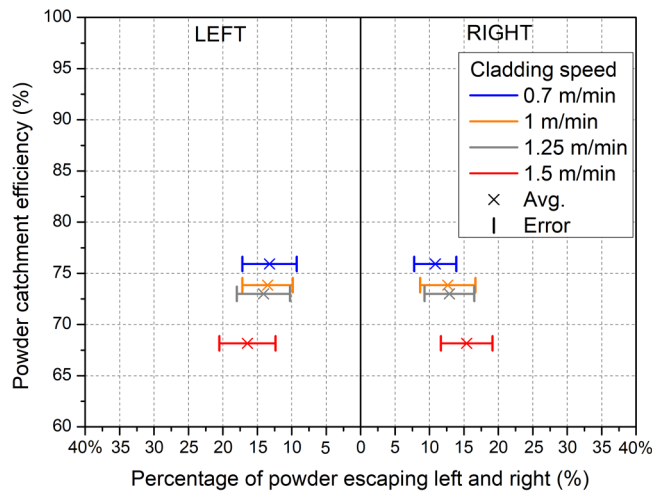


FIG. 4. Measurements of the powder catchment efficiency of single track “A” cladding as a function of cladding speed, and the proportions of particles escaping from the cladding zone in the general left and right directions.

within 2% on average, over this range of processing parameters. This extremely close fit was also evident in the other experiments carried out in this study (see Sec. III E). Given this remarkably accurate result, a great deal of care was employed to establish the error range of the results for the melt pool area measurements, the powder catchment efficiencies (cross section and particle mass) and melt pool/powder stream overlap. Each of the underlying measurements was repeated at least ten times, and the standard deviations were calculated and regarded as the error on each measurement. These were then combined to produce the overall errors given using the standard combination of error equations. The resulting errors are presented in the data boxes in Fig. 3 and other, appropriate figures.

Figure 2 suggests that particles escape from the melt pool to the right and left of the cladding path. From the HSI analysis described earlier, it was possible to quantify the proportions of particles traveling in each direction. The results of this measurement are presented in Fig. 4 and show that the two general directions of travel (left and right) were evenly matched. This is not an unexpected result as the clad track and melt pool are axi-symmetric about the axis of travel, as in the case of solo “A” clad tracks.

B. “AAA” cladding with different intertrack spacings

Standard “AAA” cladding (see Fig. 1) was carried out at a cladding speed of 0.7 m/min with intertrack spacings varied between 2 and 4 mm. Figure 5 shows a typical HSI single frame taken from the video recordings. In this case, it can be seen that the track is being overlapped with the previous one, which means

29 November 2023 10:48:07

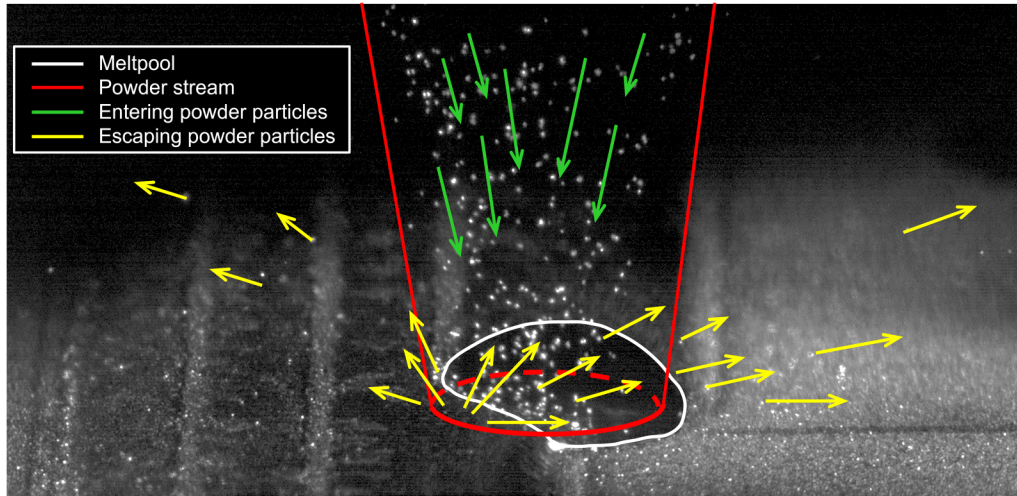


FIG. 5. A typical view of “AAA” cladding (in this case, the intertrack spacing was 2.8 mm).

that the melt pool and the surrounding area are not axially symmetrical on either side of the axis of movement as they were in the case of the single “A” track.

Figure 6 shows that, at the minimum intertrack distance (2 mm), the melt front is slightly ahead of the powder jet on the

right-hand side where the flat surface of the substrate is being clad. This could be attributed to the preheating of the area from the cladding of the previous track, as well as the effect of melt pouring downward and forward from the sloping melt pool. As the inter-track distance is increased, this preheating effect is weaker, and the

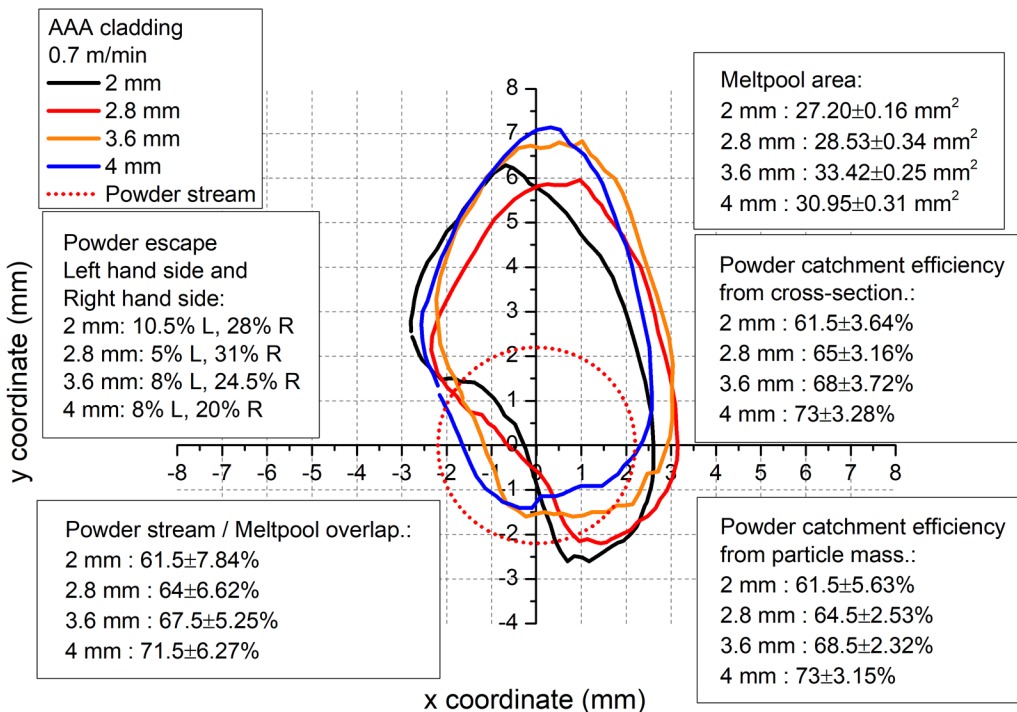


FIG. 6. Plan views of melt pools for “AAA” cladding as a function of intertrack distance. The position and size of the powder stream are indicated as a dotted circle.

29 November 2023 10:48:07

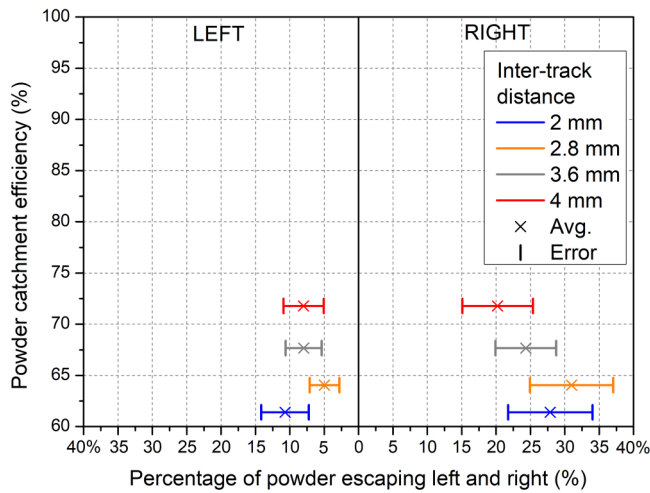


FIG. 7. Measurements of the powder catchment efficiency of “AAA” cladding as a function of intertrack distance, and the proportions of particles escaping from the cladding zone in the general left and right directions.

melt front lags the powder stream on the right-hand side as the chilling effect of the substrate becomes dominant.

On the left, the melt front substantially lags the powder stream in every case. Earlier work by the present authors⁷ suggested that this is due to the laser interacting with the curved, sloping “shoulder” of the previous track, which means that the projected beam has a lower energy density (also, other factors such as angular dependence of absorption need to be taken into account).

This distortion of the shape of the melt pool results in an increase in the percentage of powder, which impacts the

surrounding solid material. This reduces the melt pool/powder stream overlap and, thus, the powder catchment efficiency. Figure 6 demonstrates once more that these two measurements are almost exactly matched. The figures for the melt/powder overlap for this set of parameters match the powder catchment efficiency within 1.5% on average for this set of parameters.

From Figs. 3 and 6, it is clear that the powder catchment efficiency of the “AAA” process (61.5%–73%) is lower than that of single track “A” cladding (75.5%–76%) at the same cladding speed (0.7 m/min). It can also be seen from Fig. 7 that the direction of travel of the “wasted” powder particles is heavily biased toward the right-hand side. This makes sense because the “shoulder” of the previous solidified track is an inclined surface, which will tend to deflect particles toward the right.

C. “ABA” cladding with different intertrack spacings

“ABA” cladding (see Fig. 1) was also carried out at a cladding speed of 0.7 m/min with intertrack spacings varied between 2 and 4 mm.

Figure 8 shows a typical HSI single frame taken from the video recordings. The geometry of the pool in this case is symmetrical (see Fig. 1), but the geometry is rather more complex than it was for the single “A” track.

Figure 9 shows that the central part of the melt front for the “B” tracks is slightly ahead of the powder stream for ABA cladding with these parameters. This is probably because the geometry of the melt pool (caught between the two “A” tracks and sloping forwards) tends to pour liquid into the “valley” between the adjoining “A” tracks. Behind this central section, the melt pool front lags the powder stream slightly. As was the case for AAA cladding, this lag is probably caused by a reduction in the laser power density of the projected beam on the sloping surfaces of the “A” tracks. Note that in ABA cladding, preheating effects are reduced compared to “AAA” cladding. This is because, in many examples

29 November 2023 10:48:07

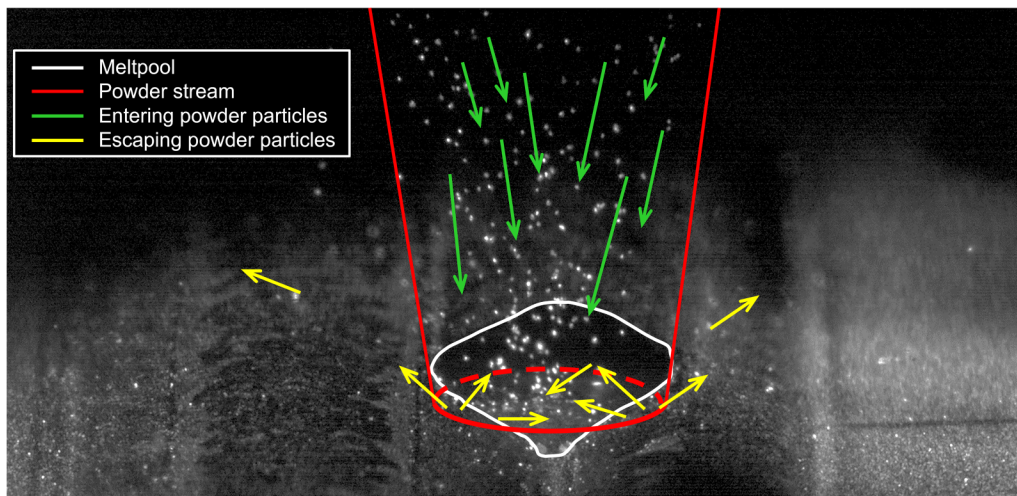


FIG. 8. A typical view of “ABA” cladding (in this case, the intertrack spacing was 2.8 mm).

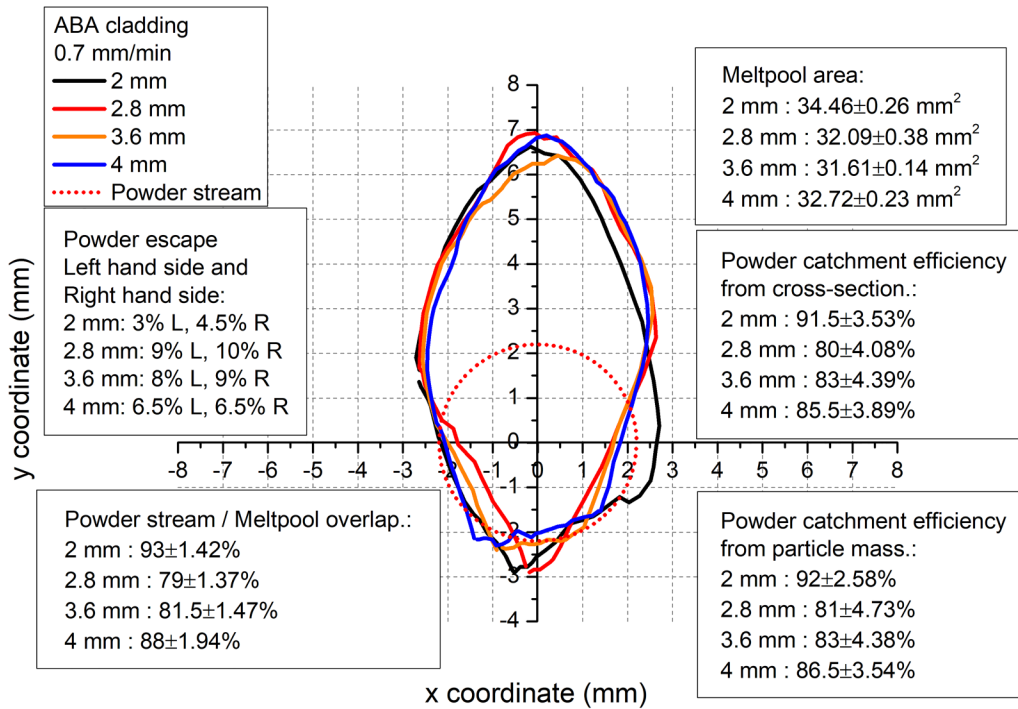


FIG. 9. Plan views of melt pools for the “B” tracks in “ABA” cladding as a function of intertrack distance. The position and size of the powder stream are indicated as a dotted circle.

of “AAA” cladding, the previous track was laid down only a few seconds earlier. In “ABA” cladding, all the “A” tracks need to be laid down before the first “B” track is clad, which gives the material time to cool down before the “B” track part of the process.

It is important to point out that Fig. 9 only gives information relating to the “B” tracks in ABA cladding. The “A” tracks were identical to those presented in Fig. 3 for a cladding speed of 0.7 m/min. Once again, we have a very accurate correlation between the powder/pool overlap (79%–93%) and the powder catchment efficiency (80%–92%), both of which are very high in the case of the “B” tracks. In the case of ABA cladding, these values are within 2% of each other on average in the cases shown here.

The powder catchment efficiency and direction of travel for ABA cladding are presented in Fig. 10 for the “B” tracks (colored lines), and it is clear that the left- and right-hand directions of powder travel are evenly balanced as a result of the symmetry of the melt pool and surrounding solid geometry (which is similar to a valley between two identical hills). Combining these results with those for the “A” tracks gives us the average values for ABA cladding, and these are presented in Fig. 10 (colored dots).

One important feature to note from Fig. 10 is the fact that even the average powder catchment efficiency of the ABA process is considerably higher (78%–83%) in the case of ABA cladding than it is for standard “AAA” cladding (61.5%–72%).

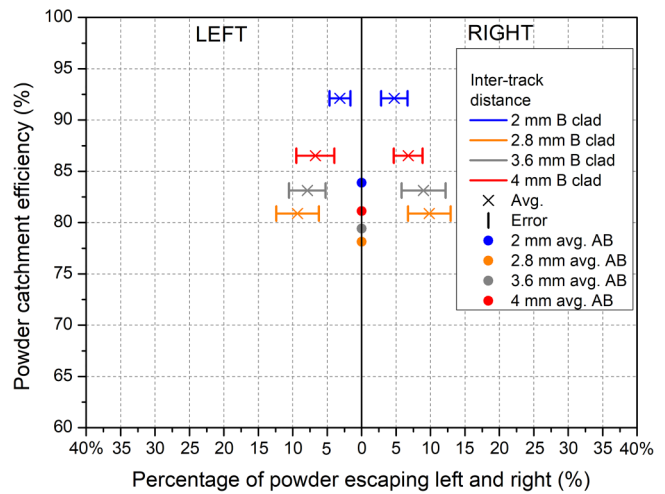


FIG. 10. Measurements of the powder catchment efficiency of “ABA” cladding as a function of intertrack distance, and the proportions of particles escaping from the cladding zone in the general left and right directions. Results for “B” tracks only (colored lines). Average results for the “ABA” process, “B” tracks plus “A” tracks, (colored dots).

29 November 2023 10:48:07

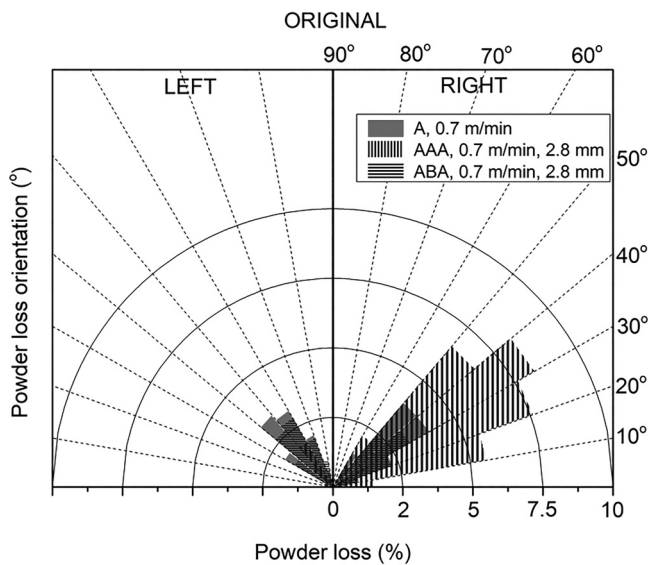


FIG. 11. A comparison of the wasted powder amounts and flight directions for “A,” “AAA,” and “ABA” cladding.

D. Comparison of the “A,” “AAA,” and “ABA” results

Figure 11 presents the data for the proportion of powder escaping the process zone and direction of travel taken, for all three types of claddings (“A,” “AAA,” and “ABA”). The information here is presented as a semicircular histogram of the proportion of powder wasted as a function of the direction of flight. For example, for “AAA” cladding, 6% of the particles rebounded at angles between 10° and 20° to the horizontal. These results demonstrate the following:

- The symmetrical flight patterns of the particles escaping from the symmetrical melt pools associated with solo “A” track and “ABA” cladding.
- The asymmetry of the escape paths for “AAA” cladding.
- More powder escapes from the “AAA” cladding process than from the solo “A” tracks, and the most powder efficient process is “ABA” cladding.

E. Summary of the “powder stream/melt pool overlap” results

Figure 12 gathers together all the experimental results above with regard to powder catchment efficiency as a function of overlap of the powder stream and the melt pool. It is clear from this figure that the correlation between the overlap and the powder catchment efficiency is very close to 100% over the range of process parameters presented here. This is an important result for the laser cladding industry as, in many cases, the process is unidirectional. This is the case, and the coaxial laser/powder stream nozzles presently in use may not be the optimum solution.

When cladding in different directions is required, coaxial systems are the obvious choice. However, for unidirectional cladding

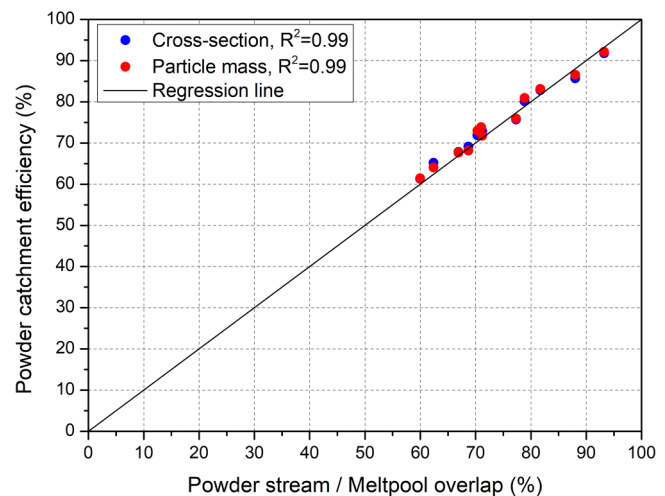


FIG. 12. The powder catchment efficiency as a function of powder stream/melt pool overlap.

(e.g., spiral cladding on tubes), the front of the melt pool can lag slightly behind the front of the laser (and the powder stream). In these cases, higher powder catchment efficiency may be achieved by employing ABA cladding or by directing the powder stream slightly backward so that it overlaps the melt pool more completely. This strategy is likely to be particularly useful at high cladding speeds where the laser/melt lag could be substantial. The possible advantage of an off-axis powder feed has also been noted by Partes.⁸

IV. CONCLUSIONS

Within the parameter set presented here, and probably more generally,

- There is an almost exact 1:1 relationship between the powder stream/melt pool overlap and the powder catchment efficiency in laser cladding (for powder streams with uniform powder flow).
- Powder catchment efficiency is maximized, for a coaxial powder feed/laser beam, by employing the ABA cladding process rather than the traditional AAA technique.
- The routes taken by particles that “escape” from the cladding process by missing the melt pool and bouncing out of the area are determined by the shape of the solid material surrounding the melt.
- To maximize profitability, laser cladding firms should maximize powder catchment efficiency by maximizing powder stream/melt pool overlap. This optimization could be achieved by techniques such as ABA cladding or by introducing a lag between the powder stream front and the front of the laser beam.

AUTHOR DECLARATIONS

Conflict of Interest

The authors have no conflicts to disclose.

Author Contributions

Daniel Koti: Writing – original draft (equal); Writing – review & editing (equal). **John Powell:** Writing – original draft (equal); Writing – review & editing (equal). **Himani Naestroem:** Writing – original draft (equal); Writing – review & editing (equal). **Chiara Spaccapaniccia:** Writing – original draft (equal); Writing – review & editing (equal). **K. T. Voisey:** Writing – original draft (equal); Writing – review & editing (equal).

REFERENCES

- ¹W. M. Steen and J. Powell, “Laser surface treatment,” *Mater. Des.* **2**, 157–162 (1981).
- ²J. Powell, “Laser cladding,” Ph.D. thesis (Imperial College London University, London, UK, 1983).
- ³P. Cavaliere, *Laser Cladding of Metals* (Springer, Berlin, 2021).
- ⁴H. S. Prasad, F. Brueckner, and A. F. Kaplan, “Powder catchment in laser metal deposition,” in *International Congress on Applications of Lasers & Electro-Optics* (AIP Publishing LLC, Melville, NY, 2018).
- ⁵H. S. Prasad, F. Brueckner, and A. F. H. Kaplan, “Powder incorporation and spatter formation in high deposition rate blown powder directed energy deposition,” *Addit. Manuf.* **35**, 101413 (2020).
- ⁶D. Koti, J. Powell, and K. T. Voisey, “Improving laser cladding productivity with ‘ABA’ cladding,” *Proc. CIRP* **111**, 205–209 (2022).
- ⁷D. Koti, J. Powell, H. Naestroem, and K. T. Voisey, “Powder catchment efficiency in laser cladding (directed energy deposition). An investigation into standard laser cladding and the ABA cladding technique,” *J. Laser Appl.* **35**, 012025 (2023).
- ⁸K. Partes, “Analytical model of the catchment efficiency in high speed laser cladding,” *Surface and Coatings Technology* **204**, 366–371 (2009).